Desalination and Water Treatment
www.deswater.com
doi: 10.5004/dwt.2019.24770

171 (2019) 331–343
December

Improvement of adsorption conditions of different parts of *Moringa oleifera* on the perception of diuron removal from contaminated waters

Héllen Karoline Spricigo de Souza[a], Márcia Regina Fagundes Klen[b], Gessica Wernke[a], Daniel Mantovani[a], Leticia Nishi[a], Quelen Letícia Shimabuku-Biadola[a], Marcelo Fernandes Vieira[a], Rosângela Bergamasco[a,*], Angélica Marquetotti Salcedo Vieira[a]

[a]*Department of Chemical Engineering, State University of Maringá, Avenida Colombo, 5790. Bloco D90, 87020–900, Maringá, Paraná, Brazil, Tel. +55 44 30114782/+55 44 30114748; emails: rbergamasco@uem.br (R. Bergamasco), karolspricigo@hotmail.com (H.K.S. de Souza), gessica.wernke@hotmail.com (G. Wernke), daniel26mantovani@gmail.com (D. Mantovani), leticianishi12@gmail.com (L. Nishi), le.shimabuku@gmail.com (Q.L. Shimabuku-Biadola), marcelofvieira@hotmail.com (M.F. Vieira), amsvieira@uem.br (A.M.S. Vieira)*
[b]*Department of Chemical Engineering, State University of West Paraná, Toledo, PR, Brazil, email: fagundes.klen@gmail.com*

Received 12 March 2019; Accepted 5 August 2019

ABSTRACT

Diuron is a herbicide that is considered potentially toxic. The conventional water treatments are not effective for its removal. Biosorption using *Moringa oleifera* emerges as an alternate process. Thus, this study evaluated Diuron's biosorption in biosorbents derivated from the fruits of *Moringa oleifera*. The biosorbents were characterised by scanning electron microscopy, Fourier transform infrared spectroscopy, textural characterisation and pH of zero load. The assays were performed in batch and evaluated the effects of parameters of contact time, pH, shaking speed, dose and granulometry of biosorbent at the biosorption process. The kinetic study was carried out, the models of pseudo-first and pseudo-second order were adjusted to the experimental data, being that the model that best fit was the pseudo-second order (q_e and R^2 in the range of 0.1339–0.1395 and 0.9849–0.9990, respectively). Adsorption isotherms were obtained at three temperatures (25°C, 35°C and 45°C) and analysed using the models Langmuir, Freundlich, Dubinin–Radushkevich and Temkin models. The model that best represented the experimental data was the Freundlich isotherm (n in the range 1.144–1.353, indicating that the biosorption is favourable). The thermodynamic properties showed that the biosorption of diuron was spontaneous and viable for the three biosorbents studied. Due to good capacity of removal of diuron (50%–74%), it can be said that the biosorbents studied are promising materials for the elimination of diuron from contaminated water.

Keywords: Biosorption; *Moringa oleifera*; Diuron; Herbicide

1. Introduction

Diuron, N-(3,4-dichlorophenyl)-N,N-dimethyl-urea, is a herbicide belonging to the family phenylamide and the subclass of phenylurea [1]. It is known as a photosystem herbicide II (PSII), which disturbs the ability of the plant to photosynthesise [2]. Several studies suggest that waters contaminated with diuron can be a precursor for the formation of nitrosodimethylamine (NDMA), composed of the family

* Corresponding author.

of N-nitrosamines, formed from the reaction of oxidation of diuron, with high carcinogenic potential [3,4].

It is observed that the contamination of water with diuron is a global concern. The import of pesticides in the first half of 2016 increased significantly from around 19.2% over the previous year. Among pesticides, the mainly imported substances are the herbicides, with a total of 111,858 tonnes according to the National Union of the Industry of Products for Plant Protection [5]. Among herbicides, the diuron is widely used for demanding crops such as cotton and sugar cane [6].

Loos et al. [7] analysed ground water samples across Europe and the frequency of detection and maximum concentrations for diuron was 29% and 279 ng L^{-1}, respectively. In a recent study, Kaonga et al. [8] verified maximum concentrations of 4.620 ng L^{-1} of diuron in water mainly due to agricultural activity, in an agricultural and urban area in Higashihiroshima City, Japan. According to the Council of the European Union [9], the maximum admissible concentration for either pesticide is 0.1 μg L^{-1} and the overall concentration allowed in drinking water is 0.5 μg L^{-1} [10]. The EU has dictated a maximum concentration of 0.1 μg L^{-1} for each pesticide and of 0.5 μg L^{-1} for all pesticides in drinking water [9,11].

The conventional water treatments are not effective in removing organochlorine pesticides, as is the case of diuron [12]. In this context, various techniques have been tested for the disposal of agricultural pesticides in waters. Among the processes, the adsorption process with activated carbon has been acquiring a high profile in this context. According to Di Bernardo Dantas et al. [10], Buchanan et al. [13] and Nam et al. [14], this technology has been successfully used for the removal of pesticides. Despite that the activated charcoal has a good adsorption capacity of agriculture inputs, the cost of these adsorbents associated to the difficulties and the high regeneration cost make its use limited in high quantity [15,16].

Thus, research has been focused on alternative adsorbents in order to try to develop low cost and efficient adsorbents, and for that they used subproducts or residues originating from agriculture or industry [16,17]. Biosorption gained important credibility for the removal of contaminants from water due to its low cost, high selectivity and excellent performance [18]. There are many studies using agricultural products as biosorbents [19–21], and among these, it is worth highlighting the *Moringa oleifera* as an adsorbent capable of removing several contaminants from water and it is possible to use its shells, pods and seeds.

The *Moringa oleifera* Lam, a plant native from northwest Indian, has been studied in several areas, such as environmental, food and medical, among others [22–25]. In terms of the water treatment application, *M. oleifera* seeds are the most studied parts of this plant, and it has been gaining attention mainly as coagulant agent [22,26]. The other parts of the fruit of *M. oleifera*, barks and pods have no relevant use and are discarded in the environment and may thus contribute to environmental pollution if not used properly. Its use as biosorbent still requires further studies, but some works achieved with our research group suggest an interesting potential of *M. oleifera* as biosorbent [27,28].

This study is based on the problem concerning the presence of diuron in waters and on the *M. oleifera* capacity to remove this kind of contaminant. Thus, the objective was evaluating the ability of the parts of the fruit (seed, bark and pods) of *M. oleifera* in biosorption process for the removal of diuron from contaminated water.

2. Experimental

2.1. Preparation of biosorbents

The fruits of *M. oleifera* were ceded by the Federal University of Sergipe (UFS), Brazil. The preparation of biosorbents is described below.

2.1.1. Seed

The seed of *M. oleifera* was separate from the bark and dried in an oven with air circulation (Sterilifer SX CR/42) to 40°C until a constant weight. Then, they were crushed in the blender and sieved in a magnetic stirrer (Bertel) in different mesh sizes of the series of Tyler sieves (850–180 μm). Thus, the biosorbent arising from the seed of *M. oleifera* was obtained. This biosorbent was called SMT.

2.1.2. Bark and pod

The bark and pod of *M. oleifera* were washed separately three times with distilled water at 60°C and dried in an oven with air circulation (Sterilifer SX CR/42) to 105°C until a constant weight. Then, they were crushed in the blender and sieved in a magnetic stirrer (Bertel) in different mesh sizes of the series of Tyler sieves (850–150 μm). These materials were used as biosorbents. The biosorbent originating from the bark of *M. oleifera* was named CSC and the biosorbent arising from *M. oleifera* pod was named VGM.

2.2. Characterisation of biosorbents

Infrared spectroscopy is used to identify functional groups in a sample, based on the vibrations of different wavelengths. The presence or absence of functional groups, their protonation states or any changes due to new interactions can be monitored by analysing the position and intensity of the different infrared absorption bands [29]. The functional groups present in parts of the fruit of *M. oleifera* before and after biosorption were evaluated by Fourier transform infrared spectroscopy (FTIR) in the range of 400 to 4,000 cm^{-1}, using a spectrophotometer Vertex 70v (Bruker®, Germany). For the evaluation of *M. oleifera* morphological characteristics, the biosorbents were characterised by scanning electron microscopy, using a scanning electronic microscope SS-550 Shimadzu Superscan (Shimadzu). The textural characterisation was done to verify the porous structure of the biosorbents arising from the parts of the fruit of the *M. oleifera*; this characterisation was performed in a system of adsorption of gases Quantachrome, by adsorption/desorption of nitrogen (N_2) to 77 K, following the basic technique recommended by IUPAC (International Union of Pure and Applied Chemistry) for characterisation of the porous structure of adsorbents. From this characterisation, the superficial area (BET method), area of micropores (method t) and the area of mesopores (BJH) of each biosorbent were obtained. In order to obtain a better understanding of the surface electrical behaviour of

the biomass particles, PZC measurements were performed to determine the pH at which the surface charges cancel out. The procedure consisted of placing in contact a mixture of 50 mg of biosorbent with 50 mL of aqueous solution under different conditions of pH, the pHs used were from 1 to 12 and the aqueous solution was adjusted with solutions of HCl and/or NaOH 1 mol L^{-1} and 0.1 mol L^{-1}, at room temperature (27°C ± 2°C), with a stirring of 180 rpm in the incubator with orbital shaking, and after 24 h, the pH was measured [30]. The PH_{pzc} corresponds to the pH value at which the curve ΔpH vs. initial pH intercepts the x axis ($y = 0$), in which ΔpH is the difference between the initial and the final pH.

2.3. Biosorption experiments

All experiments of biosorption of this work were performed in each batch. The study of biosorption was performed according to the methodology of Gupta et al. [31].

For these experiments, the quantity of diuron adsorbed by biosorbents studied, q_e (mg g^{-1}), was calculated by the following equation:

$$q_e = \frac{V.\left(C_0 - C_{eq}\right)}{m} \quad (1)$$

where C_0 is the initial concentration of diuron in solution (mg L^{-1}), C_{eq} is the concentration of diuron on balance (mg L^{-1}), V is the volume of solution (L) and m is the mass of biosorbent (g).

From the biosorption experiments, the following were evaluated: equilibrium time, mass and granulometry of biosorbent, shaking speed, pH, temperature, kinetics of biosorption, biosorption isotherms and thermodynamic parameters. The methodology for each of these analyses and also the preparation of a solution contaminated with diuron is described as follows.

2.3.1. Equilibrium time

To estimate the equilibrium time, a study of the contact time between each of the biosorbents and the adsorbate was carried out. The study was conducted by setting the temperature of 25°C, the granulometry of the adsorbent, between 500 and 600 μm, the adsorbent mass of 0.5 g, stirring speed of 100 rpm, volume of contaminant solution of 25 mL and pH 6.5. The initial concentration of diuron was 5 mg L^{-1}. The experiment was performed in an incubator with orbital shaking for 24 h. The samples were collected in several time intervals, filtered in filter of cellulose acetate 0.45 μm porosity and analysed in high performance chromatography (HPLC).

2.3.2. Statistical analysis

Bearing the contact time necessary to establish the equilibrium time, the following parameters were evaluated: granulometry of biosorbent, shaking speed, pH, temperature and mass of biosorbent. It was used a randomised trial (randomised Plackett–Burman), which allows the identification of variables that impact significantly in the process of adsorption. The design of the planning was 2^4 with central point. The assays were performed in duplicate and the central point was performed in three replicas. In Table 1 the parameters that were evaluated are presented.

From the experimental data, a statistical analysis of variance (ANOVA one way) was performed in order to check which effects were significant in the process of adsorption of diuron. The effects are significant when p-value < 0.05 with a confidence level of 95%.

2.3.3. Biosorption kinetics

To evaluate the adsorption kinetics, 25 mL of diuron at 5 mg L^{-1}, 0.5 g adsorbent, a stirring speed of 200 rpm, temperature of 25°C, pH 10 and a particle size of 500 μm was used. After the experimental results were obtained, kinetic models of pseudo-first order [32], pseudo-second order [33] and intraparticle diffusion [34] (Eqs. (2)–(4), respectively) were adjusted

$$q_t = q_{eq}\left[1 - \exp\left(-k_1 t\right)\right] \quad (2)$$

$$q_t = \frac{k_2 q_e^2 t}{1 + k_2 q_e t} \quad (3)$$

$$q_t = K_d t^{1/2} + C \quad (4)$$

where q_t is biosorption capacity at time (mg g^{-1}); q_e is biosorption capacity at equilibrium (mg g^{-1}); t is reaction time (min); k_1 is biosorption rate constant of pseudo-first order (min^{-1}); k_2 is biosorption rate constant of pseudo-second order (g mg^{-1} min^{-1}); K_d is intraparticle diffusion coefficient (mg g^{-1} $min^{-1/2}$); C is a constant related to diffusion resistance (mg g^{-1}).

In order to check whether surface diffusion controls the adsorption process, the kinetic data were further analysed using Boyd kinetic expression which is given by Boyd et al. [35]:

$$F = 1 - \frac{6}{\pi^2}\exp(-B_t) \quad \text{or} \quad B_t = -0.4977 - \ln(1 - F) \quad (5)$$

where $F(t) = q_t/q_e$ is the fractional attainment of equilibrium at time t, and B_t is a mathematical function of F.

Table 1
Plackett and Burman planning: screening of 2 levels + central point

Factors	Levels		
	(–1)	(0)	(+1)
Mass of biosorbent (g)	0.1	0.3	0.5
Granulometry (mm)	0.150	0.300	0.500
pH	4	7	10
Temperature (°C)	25	35	45
Shaking speed (RPM)	100	150	200

2.3.4. Biosorption isotherms

For biosorption isotherms, the initial concentration of diuron ranged from 2 to 41 mg L^{-1}. A mass of biosorbent of 0.5 g, granulometry of 500 μm, solution pH initial 10 and stirring speed of 200 rpm was used. The data of the balance tests were obtained in three temperatures: 25°C, 35°C and 45°C. For the data of adsorption isotherms, the models of Langmuir [36], Freundlich [37], Temkin [38] and Dubinin–Radushkevich [39] were adjusted according to Eqs. (6)–(9), respectively.

$$q_e = \frac{q_m \cdot b_L \cdot C_e}{1 + b_L \cdot C_e} \tag{6}$$

$$q_e = k_F \cdot C_e^{1/n} \tag{7}$$

$$q_e = \frac{RT}{b} \ln\left(K_T C_e\right) = B_1 \ln\left(K_T C_e\right) \tag{8}$$

$$q_e = q_m \exp\left(-K\left[RT \ln\left(1 + \frac{1}{C_e}\right)\right]^2\right) = q_m \exp\left(-K\varepsilon^2\right) \tag{9}$$

where q_m is the maximum capacity of adsorption (mg of diuron/g of *M. oleifera*); b_L is the constant of Langmuir isotherm (L mg^{-1}); C_e is the equilibrium concentration of diuron in the solution (mg L^{-1}); q_e is the amount adsorbed (mg g^{-1}); K_F is the constant of Freundlich isotherm that is related with the affinity of adsorption (mg L^{-1}) (L $g^{-1})^{1/n}$; n is a constant characteristic related to intensity or degree of adsorption favourability in the Freundlich equation; $B_1 = RT/b$ and is related to the heat of adsorption; R is the Universal gas constant (J mol^{-1} K^{-1}); T is the temperature (K); b is the energy variation of adsorption (J mol^{-1}); K_T is the equilibrium binding constant (L mg^{-1}) corresponding to the maximum binding energy; ε is the Polanyi potential, which is equal to $RT \ln(1 + 1/C_e)$; K is the constant energy of adsorption in mol^2 kJ^{-2} and is related to the average energy of sorption (E).

The average energy of sorption (E) can be calculated as follows [39]:

$$E = \frac{1}{\sqrt{2K}} \tag{10}$$

2.3.5. Thermodynamic parameters

For the calculation of the thermodynamic parameters (Gibbs free energy (ΔG), enthalpy (ΔH) and entropy (ΔS)) concentrations of 2–41 mg L^{-1} of diuron at temperatures of 25°C, 35°C and 45°C, a stirring speed of 200 rpm, pH 10 and 0.5 g of biosorbent were used.

The enthalpy and entropy were calculated by the following equation [40]:

$$\ln K_c = -\frac{\Delta H}{RT} + \frac{\Delta S}{R} \tag{11}$$

where ΔH is the enthalpy (kJ mol^{-1}), ΔS is the entropy (kJ mol^{-1} K^{-1}) and K_c is the constant of balance which is given by q_e/C_e [41]. The values of ΔH and ΔS are calculated by plotting ln K_c vs. $1/T$. The Gibbs free energy (ΔG) in kJ mol^{-1}, was estimated using Eq. (12):

$$\Delta G = -RT \ln K_c \tag{12}$$

where R is the constant of gases in kJ mol^{-1} K^{-1} and T is the temperature in K.

2.3.6. Analysis in high performance liquid chromatography

The solutions containing diuron were prepared from the commercial product 500 g L^{-1} (500 SC, Nortox, Brazil) in reverse osmosis water. All samples obtained in experiments of biosorption were analysed in HPLC. For these analyses, Gilson trademark equipment was used while controlled by Software Born, equipped with manual injector Rheodyne, with a volume of injection of 20 μL, pump model 307 and UV/Visible detector model 151, with reading at 247 nm. The analysis was conducted using as mobile phase acetonitrile/water with relation (65/35) and column Microsorb-MV (5 μm, 100 Å; 4.6f–250 mm), with a flow rate of 0.75 mL min^{-1} at temperature of 35°C. The determination of the concentration of diuron was estimated considering a calibration curve obtained between 0.05 and 42 mg L^{-1}, with R^2 of 0.9958 and linear regression equation expressed by:

$$C_d = 9 \times 10^{-6} A + 0.0489 \tag{13}$$

where C_d is the concentration of diuron in mg L^{-1} and A is the peak area.

3. Results and discussion

3.1. Characterisation of biosorbents

Studies of characterisation of the biosorbents of *M. oleifera* are of great value in the interpretation and clarification of the results associated with the properties of these biomaterials.

3.1.1. Scanning electron microscopy

The morphology of biosorbents was investigated by means of scanning electronic microscopy. The images were obtained using 300 times magnification. Micrographs of biosorbents can be seen in Fig. 1.

By means of Fig. 1, it can be observed that the three materials present very heterogeneous morphological characteristics. The CSC and VGM biosorbents are relatively porous, and now SMT presents a dense characteristic. These characteristics are due to the fact that parts of the fruit of the *M. oleifera* (bark, seed and pod) possess a great variety of components that comprise its biomass. For the three biosorbents, the presence of malformations in the surface of the plant tissue are visible, containing the available spaces that allow favourable conditions for adsorption of metal or organic chemical

species in their interstices when these materials are used as biosorbents [42]. It is observed that the biosorbents CSC and VGM have quite fibrous characteristics; this is due to the chemical constitution of those materials that are rich in lignin and cellulose.

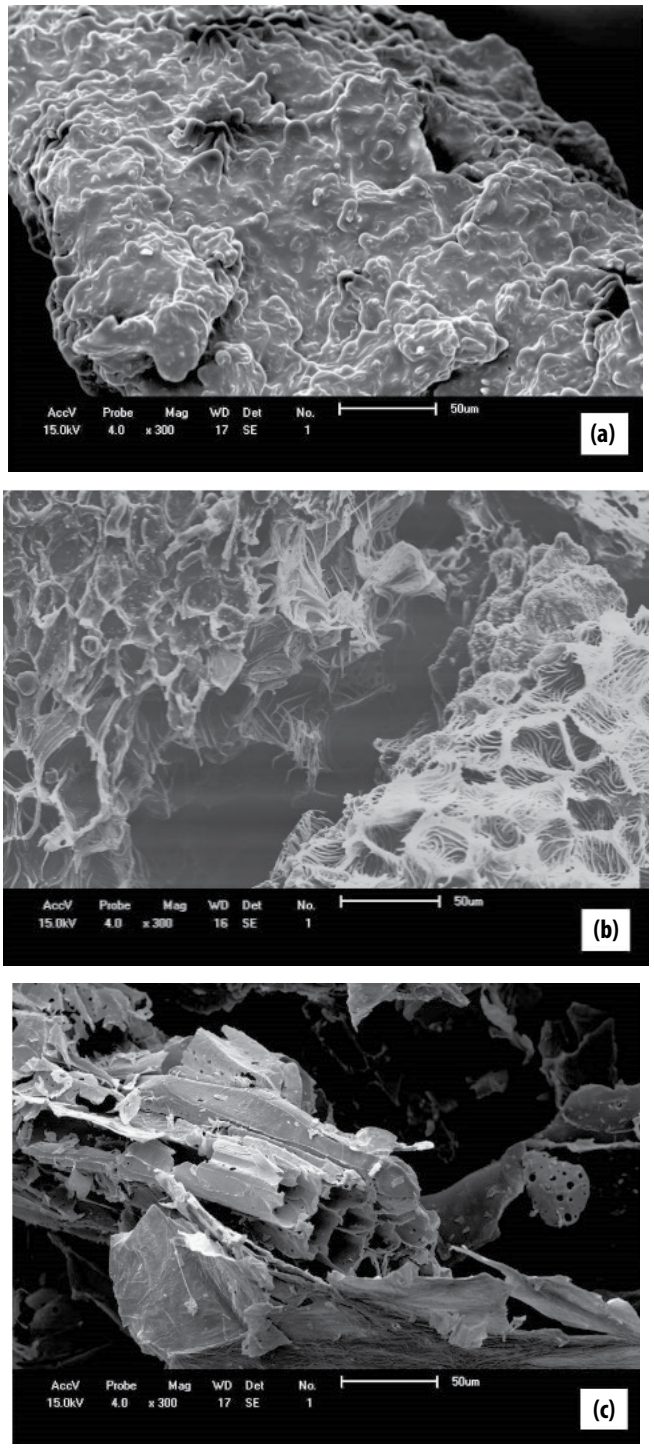

Fig. 1. Scanning electronic microscopy. Magnitude 300x. (a) SMT, (b) CSC and (c) VGM.

3.1.2. Textural characterisation Brunauer–Emmett–Teller (BET)

To evaluate the adsorptive characteristics of the biosorbents originating from parts of the fruit of *M. oleifera*, analyses of textural characterisation were performed. With these analyses, it was possible the determination of specific surface area, area of micropores and mesopores of each one of the studied biosorbents. The values of textural properties for the biosorbents SMT, CSC and VGM are presented in Table 2.

By means of Table 2 it can be observed that the superficial area of biosorbent VGM (44.05 $m^2 g^{-1}$) was greater than that of the CSC (36.09 $m^2 g^{-1}$) and of the SMT (18.93 $m^2 g^{-1}$). The three biosorbents contain in their structure micropores and mesopores. Comparing the area of micropores and mesopores, it appears that for the VGM the area of micropores and mesopores was close, now for the CSC and SMT there is a greater quantity of mesopores.

Akhtar et al. [21] studied the superficial area of the pod of *M. oleifera*, with value found of be 16 $m^2 g^{-1}$. It is verified that this author got an area smaller than that found for the biosorbent arising from the pod (VGM) in this work, but he also found a predominance of mesopores.

3.1.3. Point of zero charge (PZC)

The point of zero charge of each biosorbent corresponds to the pH in which the total charge is zero. At the pH below the pH of point of zero charge (pH_{pzc}), the surface of the biosorbent is positive, whereas above this value, it is negative [43]. The pH_{PZC} observed for SMT was 6.62, for CSC, it was 7.39 and for VGM, 7.52. Thus, in pH greater than 6.62 (SMT), 7.39 (CSC) and 7.52 (VGM), these biomaterials are negatively charged, possessing the ability to adsorb species positively charged, while below these values of pH, these biosorbents are charged positively and will preferably adsorb species negative.

Diuron is a non-ionic herbicide [44]. According to Rocha et al. [45], non-ionic herbicides can be polar and, in virtue of this condition, be affected by pH. These authors studied the sorption and desorption of diuron in four Brazilian latosoils and observed that the increase of soil pH increased sorption of diuron. Thus, only if the diuron detaches, the pH will be influencing at the biosorption and, if this happens, the best pH for the biosorption will depend on the load gained by diuron.

3.1.4. Infrared spectroscopy with Fourier transform (FTIR)

According to Madhava Rao et al. [46], the adsorption process promoted by biomasses depends more strongly on the presence of reactive functional groups in the surface area of

Table 2
Textural properties of the biosorbents SMT, CSC and VGM

	SMT	CSC	VGM
Surface area ($m^2 g^{-1}$)	18.93	36.09	44.05
Area of mesopores ($m^2 g^{-1}$)	14.72	28.12	29.02
Area of micropores ($m^2 g^{-1}$)	4.60	10.04	25.85

the particles than the superficial area or other parameter of surface.

The knowledge of the functional groups present in biosorbent materials should help understand the biosorption mechanisms. The biosorbents originating from the *M. oleifera* fruit were characterised by the technique of FTIR before and after the biosorption process. For the analysis before the biosorption, a sample with a particle size of 500 μm was used. For the post-biosorption sample, pH 10, stirring at 200 rpm, temperature of 25°C, 0.5 g of mass of biosorbent, particle size of 500 μm and concentration of 5 mg L^{-1} of diuron were used. The results obtained are shown in Fig. 2.

The spectra of FTIR before and after the diuron biosorption show the presence of various functional groups, indicating the complex nature of the parts of *M. oleifera* fruit. For the biosorbents SMT, CSC and VGM, the large band in the region of 3,200–3,500 cm^{-1} may be attributed to the stretching of connections OH present in proteins, fatty acids, carbohydrates and lignin [42]. According to studies by Reddy et al. [47], the peaks present in SMT at 2,926 cm^{-1}, in the CSC at 2,924 cm^{-1}, and in VGM at 2,918 cm^{-1} are due to the presence of asymmetric stretching of aliphatic chains (C–H) present in organic compounds. According to Pan and Guan [48], the peaks between 2,843 and 2,863 cm^{-1} refer to symmetric stretching vibration of CH_2; in SMT this peak appears at 2,854 cm^{-1} and in CSC at 2,855 cm^{-1}. The peaks 1,746 and 1,655 cm^{-1} present in biosorbent CSC, and 1,736 and 1,635 cm^{-1} presents in biosorbent VGM, referring to the stretching of connection C=O, which is what is present in the hemicellulose and lignin. Already the peak at 1,653 cm^{-1} is regarding the presence of amide groups that are present in proteins. The at peak 1,059 cm^{-1} in CSC and 1,053 cm^{-1} in VGM corresponds to the asymmetric stretching of the connection C-O-C, which includes compounds such as carboxyl groups which confirms the structure of lignin [23].

The possible changes observed between the spectra before and after the biosorption, for all the biosorbents, are due to electrostatic interactions between functional groups of the biosorbent and the contaminant groups, leading to small changes in the spectrum of a general manner.

3.2. Biosorption assays

The biosorption first stage of the study was to analyse the contact time between the biosorbent and the adsorbate during 24 h. The study was carried out in a batch and was conducted by fixing the adsorbent particle size of 500 μm, the adsorbent mass of 0.5 g, the agitation speed of 100 rpm, the volume of 25 mL of contaminant solution and the temperature of 25°C, with pH 6.5. Fig. 3 shows the result obtained for the three biosorbents.

From Fig. 3 it is observed that the adsorption of diuron increases drastically in the first 10 min. This is due to the presence of a large number of empty places. As time increases, the adsorption of diuron increases, but less intensely due to the accumulation of this vacant sites of the adsorbent. Observing the results obtained, we can verify that with 60 min, the state of equilibrium for the three biosorbents is established.

After determining the time for the state of balance for each biosorbent, experimental planning has been performed

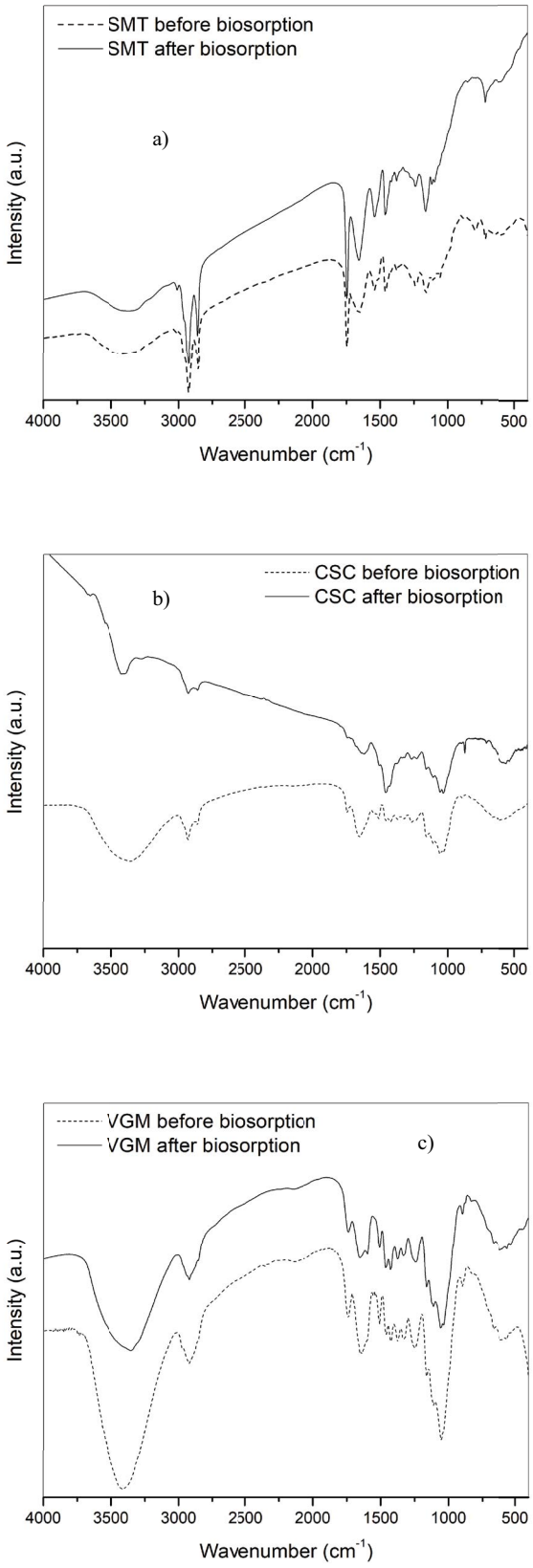

Fig. 2. Mass spectrometers obtained through FTIR of biosorbents SMT (a), CSC, (b) and VGM (c) before and after diuron's biosorption.

to determine which variables have relevant effects on the process of biosorption.

In Table 3 the parameters and their respective *p*-value and effects are presented. When the effect is positive it means that the answer is increasing as the factor assessed increases, and when it is negative, it means that the answer is increasing as the evaluated factor decreases. The parameters that were considered significant for the adsorption have *p*-value < 0.05.

It is observed in Table 3 that the parameters that are significant for the biosorbent SMT in biosorption diuron (*p*-value < 0.05) are the mass of biosorbent, temperature and shaking speed. The granulometry of the biosorbent and the initial pH of the solution were not significant, that is, the biosorption of diuron by the biosorbent SMT is not dependent on these factors. Still in Table 3 it is possible to check that the effect is positive for the parameters that were significant, denoting that the greater this factor greater will be the removal of diuron.

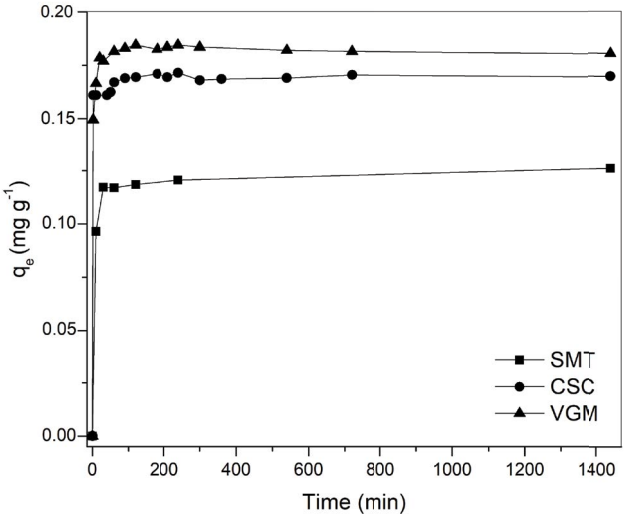

Fig. 3. Evaluation of balance time of biosorbents SMT, CSC and VGM.

Table 3
Statistical analysis of parameters that influence the diuron's biosorption

Biosorbent	Parameters	*p*-value	Effect
SMT	Mass of biosorbent (g)	0.000000	27.56
	Granulometry (mm)	0.102938	–2.83
	pH	0.292660	1.79
	Temperature (°C)	0.000000	10.75
	Shaking speed (rpm)	0.006504	4.89
CSC	Mass of biosorbent (g)	0.000000	32.54
	Granulometry (mm)	0.998810	–0.00195
	pH	0.049506	2.64
	Temperature (°C)	0.161226	–1.85
	Shaking speed (rpm)	0.007949	3.67
VGM	Mass of biosorbent (g)	0.000000	32.20
	Granulometry (mm)	0.272283	–1.49
	pH	0.001275	4.72
	Temperature (°C)	0.448245	–1.02
	Shaking speed (rpm)	0.890508	0.1837

The parameters that are significant for the biosorbent CSC in biosorption of diuron (*p*-value < 0.05) are mass of biosorbent, pH and shaking speed. The granulometry of biosorbent and the temperature was not significant.

Now for the biosorbent VGM, significant parameters in the adsorption of diuron (*p*-value < 0.05) are the mass of biosorbent and the pH. The granulometry of the biosorbent, temperature and shaking speed was not significant, that is, the biosorption of diuron by the biosorbent VGM is not dependent on these factors.

The granulometry of biosorbents was not significant for any biosorbents used. This is not usually the case, since the lower the particles the greater the contact area between the biosorbent and the contaminated solution and thus the greater the biosorption. This fact is probably due to the microporous and mesoporous characteristics, besides the heterogeneity of biosorbents.

The mass was the parameter that had the greatest effect for the three biosorbents, and the greater the mass, the greater was the diuron's biosorption. As the concentration of the biosorbent increases, the number of available sites also increases, so more ions of the adsorbate may be adsorbed to the surface of the adsorbent, and with this, there is an increase in the removal of diuron.

For the CSC and VGM biosorbents, a greater removal increasing the pH was possible. As already observed by the analysis of pH_{pzc}, at pH 10 the surface of the CSC and VGM are charged negatively and can also have occurred to the presence of more hydroxyl ions due to the decoupling of different functional groups present in these biosorbents, besides the polarisation of diuron (Rocha et al. [45], thus resulting in an increase of the adsorption of diuron by surface of VGM and CSC biosorbent at a higher pH. As the surface of the CSC and VGM biosorbents are charged negatively, probably diuron polarized and acquired positive charge that there is among the biosorbent (CSC and VGM) and diuron in an ionic interaction. For the SMT biosorbent, pH was not a significant parameter in the biosorption of diuron. This is probably due to the functional groups present in the SMT biosorbent not to dissociate in the pH range studied and diuron not to polarize. Thus, as there was no significant difference for the removal of diuron regardless of the load of biosorbent (positive, negative or zero), a hydrophobic interaction between the diuron and the SMT biosorbent is likely to occur.

For the SMT biosorbent, there was an increase in the removal of diuron with the increase of temperature. According to the studies carried out by Mataka et al. [49] with the seed of *M. oleifera*, which is the material used for the preparation of the SMT biosorbent, as the temperature is increased, a number of connections in the polypeptides, which are the agents of sorption suggested, are weakened. This affects long-range interactions that are necessary for the presence of tertiary structure. With these connections weakened and broken, the polypeptide is with a more flexible structure and the groups are exposed to the solvent. This

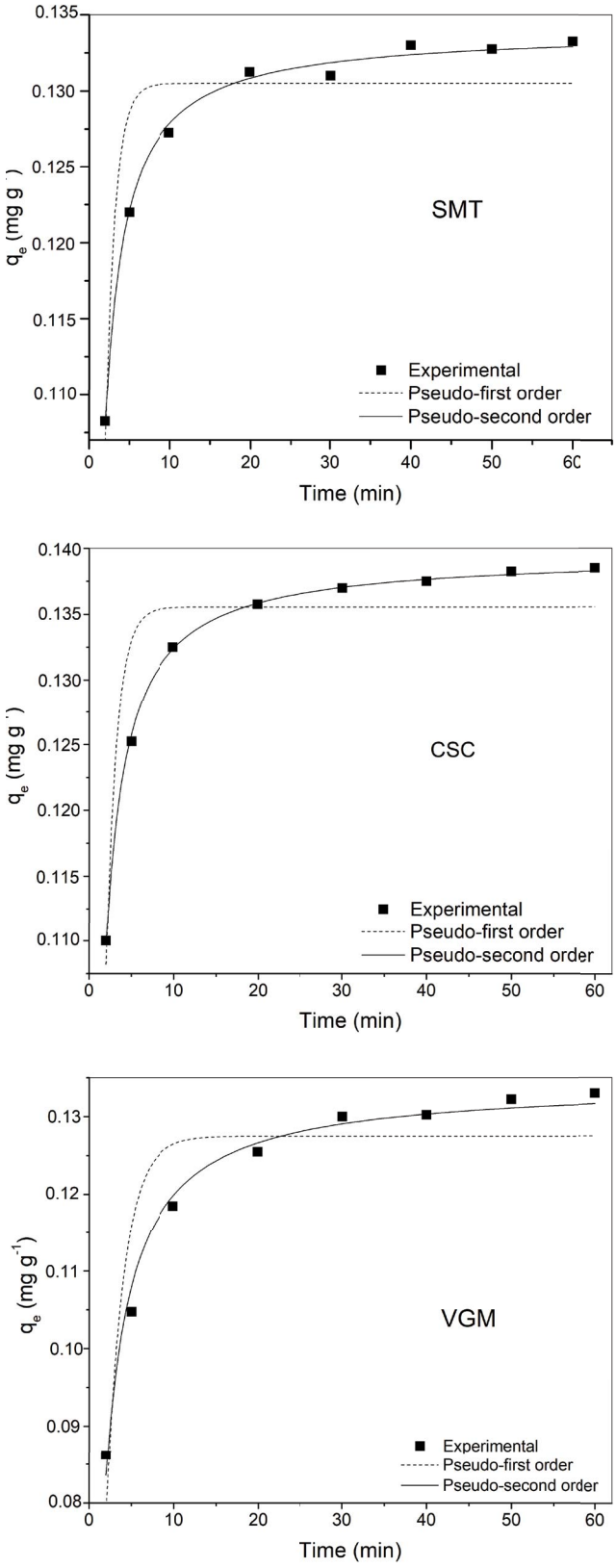

Fig. 4. Biosorption kinetics of diuron for SMT, CSC and VGM biosorbents applying models of pseudo-first and pseudo-second order models.

exposure of more groups to the solvent presumably increases the number of binding sites for higher sorption of diuron.

Depending on the value used, the stirring speed can influence the process of biosorption. When the mass transfer is the limiting factor of the process and if the speed of agitation increases, decreasing the boundary layer, the resistance of the film mass transfer surrounding the particles of biosorbent is decreased, causing an increase in the adsorbate biosorption [50]. For the biosorbents SMT and CSC, the shaking speed had influence in the efficiency of biosorption of diuron; the more agitated the solution and the solute, the greater were the agitation of the particles biosorbent and the molecules of adsorbate in solution, thus resulting in a decrease of the boundary layer and increase the chance of having a greater biosorption.

The maximum removal of diuron achieved in the experiments of experimental planning for the determination of the parameters that are significant in biosorption of diuron was 68% for the biosorbent SMT, which corresponds to a final concentration of diuron in solution of 1.67 mg L^{-1}; 63% for the biosorbent CSC, corresponding to 1.86 mg L^{-1} of diuron in solution and for the biosorbent VGM 64% was obtained corresponding to 1.88 mg L^{-1} of final concentration of diuron in solution.

After the statistical analysis, the parameters used in the next steps (kinetics and adsorption isotherms) were pH 10, stirring speed of 200 rpm, temperature of 25°C, biosorbent mass of 0.5 g of and particle size of 500 μm. Even with the pH not being significant for the biosorption of diuron by the SMT biosorbent, we opted, for comparison purposes, to use the same pH for all biosorbents studied.

3.2.1. Kinetic studies

The adsorption kinetics determines the evolution of the adsorption capacity in relation to time and is necessary for identifying the type of adsorption mechanism that occurs in a given system [58].

To evaluate adsorption kinetics, 25 mL of 5 mg L^{-1} diuron solution, 0.5 g of adsorbent, 200 rpm stirring speed, 25°C, pH 10 and a particle size of 500 μm were used. Figs. 4 and 5 present the adjustments to pseudo-first-order, pseudo-second-order and intraparticle diffusion models. The experimental results in the kinetics of biosorption are shown in Table 4.

The model that best fits to the experimental data obtained for the three biosorbents was the pseudo-second order model. The correlation coefficient of the pseudo-second order model was greater than for the pseudo-first order model for the three biosorbents studied and the estimated value of q_e for this model was also near the experimental value (q_{exp}). Both factors suggest that the biosorption of diuron for the three studied biosorbents follows the kinetic model of pseudo-second order. According to Febrianto et al. [51], if compared the kinetic model of pseudo-first, pseudo-second order and intraparticle diffusion, the pseudo-second order model is considered more appropriate to represent the kinetic data in biosorption systems. The pseudo-second order model is used to describe chemisorption involving forces of valence through sharing or exchange of electrons between biosorbent and adsorbate, as forces covalent bonds and ion exchange [52].

In the case of the intraparticle diffusion model, if the only rate-limiting step is intraparticle diffusion, q_t vs. $t_{1/2}$ must be a straight line through the origin [53]. Fig. 5 indicates that the adsorption process is controlled by more than one site, for all the studied adsorbents, since they exhibit data with adjustments that are not linear over the entire studied time frame. The first part gives the diffusion through the solution to the external surface of adsorbent or boundary layer diffusion. The second linear portion is attributed to the gradual equilibrium stage with intraparticle diffusion dominating. The third portion is the final equilibrium stage for which the intraparticle diffusion starts to slow down due to the extremely low adsorbate concentration left in the solution [54]. In this work, two adsorption zones are observed, attributed to adsorption on the external surface and intraparticle diffusion. For the SMT and CSC adsorbents, the correlation coefficients ranged from 0.7589 to 0.9721, thus being below the R^2 value for the pseudo-second order model, indicating that the intraparticle diffusion kinetic model does not effectively explain the observed adsorption process.

Table 4
Biosorption kinetics of SMT, CSC and VGM biosorbents

	SMT	CSC	VGM
Pseudo-first order			
q_{exp} (mg g^{-1})	0.1333	0.1385	0.1330
q_e (mg g^{-1})	0.1305	0.1356	0.1275
k_1 (min^{-1})	0.8562	0.8005	0.4810
R^2	0.8274	0.8364	0.8087
Pseudo-second order			
q_e (mg g^{-1})	0.1339	0.1395	0.1343
k_2 (g mg^{-1} min^{-1})	15.53	13.20	6.1394
R^2	0.9958	0.9990	0.9849
Intraparticle diffusion			
K_d (mg g^{-1} min$^{-1/2}$) (Zone I)	0.0108	0.0128	0.0184
C (mg g^{-1}) (Zone I)	0.0947	0.0936	0.0614
R^2 (Zone I)	0.9198	0.9449	0.9858
K_d (mg g^{-1} min$^{-1/2}$) (Zone II)	0.0007	0.0008	0.0022
C (mg g^{-1}) (Zone II)	0.1279	0.1322	0.1168
R^2 (Zone II)	0.7589	0.9721	0.9079

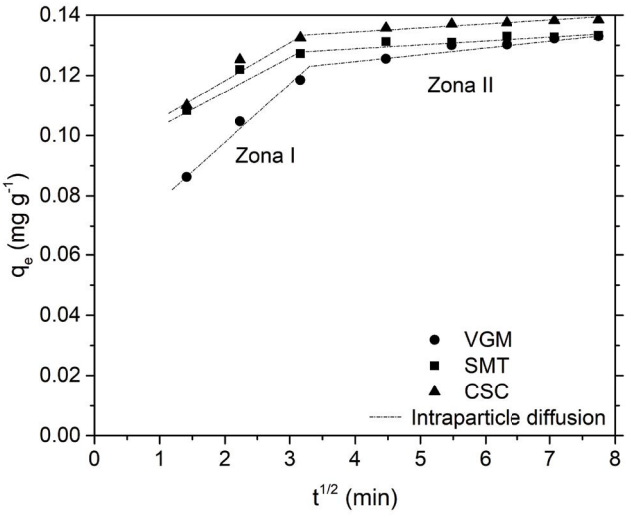

Fig. 5. Adjustment of experimental data to kinetic models of intraparticle diffusion.

In the case of the adsorbent VGM, R^2 was obtained for Zone I, close to R^2 found for the pseudo-second order model. To verify if intraparticle diffusion controls the adsorption process for the VGM adsorbent, the Boyd equation was applied. The line generated by the graph B_t vs. t (not shown) does not pass through the origin ($y = 0.0781x + 0.6849$, $R^2 = 0.9661$), confirming that intraparticle diffusion is not responsible for total process control. Thus, and as a function of the previously discussed, it is understood that this non-kinetic model does not represent the adsorption of diuron on the adsorbent VGM.

Thus, for the three studied biosorbents, the biosorption process can be controlled by chemisorption involving force of valence through sharing or exchange of electrons between biosorbents originating from the parts of the fruit of *M. oleifera* and diuron.

3.2.2. Adsorption isotherms

After performing the kinetic study, the isotherms of balance were studied. The isotherms were obtained at three temperatures: 25°C, 35°C and 45°C. To assess which model of isotherm best fits to the data obtained, we used the Langmuir, Freundlich, Dubinin–Radushkevich (D-R) and Temkin models. The parameters for the isothermal models analysed are shown in Table 5.

Langmuir and Freundlich were the two models that presented better adjustments for the three temperatures. In Fig. 6 the graphics with the models that best adjusted to the experimental data in each of the temperatures studied (Freundlich and Langmuir) are presented.

It is suggested that the model that best describes the biosorption process for the studied biosorbents is Freundlich's, since the three biosorbents (SMT, CSC and VGM) are very heterogeneous materials, as verified by scanning electron microscopy photos (Fig. 1). Some authors who worked with biosorbents also found Freundlich to be the best model to describe the biosorption process. It can be mentioned that Ebrahimi et al. [53] used *Alhagi maurorum* for cadmium removal; Srivastava et al. [54] used *Lagerstroemia speciosa* bark for Cr(VI) removal; Wang et al. [55] used *Pinus massoniana* for uranium removal.

The Freundlich equation implies that the distribution of energy to the sites of biosorption is essentially exponential, instead of being uniform type as considered in the development of the Langmuir equation. According to Cooney [56], there are experimental evidences that the distributions of energy might not be strictly exponential. It is considered that some sites are highly energetic and the connection of the solute adsorbed is given strongly, while some are much less energetic, and consequently, the connection is given weaklier.

The value of n in the Freundlich isotherm at the three temperatures and for the three biosorbents analysed is between 1 and 10, thus indicating that the biosorption is favourable [19].

Table 5
Parameters obtained for adsorption isotherms for the SMT, CSC and VGM

Isotherm model	SMT			CSC			VGM		
	25°C	35°C	45°C	25°C	35°C	45°C	25°C	35°C	45°C
Langmuir									
q_{max} (mg g^{-1})	2.290	2.345	2.350	5.784	5.554	5.152	3.761	3.454	2.994
b (L mg^{-1})	0.040	0.046	0.051	0.021	0.020	0.020	0.028	0.029	0.033
R^2	0.997	0.995	0.995	0.995	0.995	0.992	0.996	0.994	0.995
Freundlich									
k (mg g^{-1})	0.110	0.128	0.140	0.134	0.123	0.117	0.130	0.125	0.123
N	1.318	1.337	1.353	1.144	1.151	1.167	1.248	1.272	1.300
R^2	0.994	0.993	0.991	0.993	0.993	0.993	0.999	0.999	0.998
D-R									
q_m (mg g^{-1})	0.910	0.995	1.001	1.340	1.278	1.148	1.185	1.148	1.093
K (mol^2 kJ^{-2})	3.790	3.327	2.844	4.011	4.258	3.057	3.999	4.290	3.755
E (kJ mol^{-1})	0.363	0.388	0.419	0.363	0.343	0.404	0.355	0.341	0.365
R^2	0.895	0.907	0.905	0.921	0.899	0.897	0.900	0.893	0.898
Temkin									
b (J mol^{-1})	7,734	9,066	9,096	5,974	6,175	6,375	7,468	8,169	8,688
K_T (L mg^{-1})	0.822	1.324	1.474	1.134	1.139	1.047	1.341	1.429	1.389
R^2	0.934	0.882	0.909	0.904	0.883	0.886	0.867	0.885	0.887

3.2.3. Thermodynamic parameters

When isotherms at different temperatures are offered, it is possible to estimate the thermodynamic parameters (ΔG, ΔH and ΔS). The values of ΔH, ΔS and ΔG are shown in Table 6. The graphs of ln K_c vs. $1/T$ used for the estimation of thermodynamic parameters are presented in Fig. 7.

A higher negative value to ΔG reflects a more energetically favourable adsorption. The positive value of $\Delta H°$ implies that adsorption would be an endothermic process, where as a negative $\Delta H°$ indicates an exothermic adsorption process. A low $\Delta S°$ value often signifies no remarkable change in entropy during adsorption, whereas a positive $\Delta S°$ value reflects the increased randomness at the solid–solution interface during adsorption [40].

From Table 6 it is verified that for the three biosorbents the value of ΔG is negative; this indicates the viability of the process and the spontaneous nature of biosorption in the three temperatures studied. For the biosorbent SMT, the value of ΔH is positive, indicating that the biosorption process that occurs between the SMT and diuron is a process that absorbs heat, and it is soon an endothermal process. In the evaluation of the parameters that influenced the adsorption of diuron by SMT, it was verified that the temperature increase favoured the removal of diuron, which fits in with the result of endothermic process found with the biosorbent SMT. Now for the CSC and VGM biosorbents, ΔH is negative, indicating that the process of biosorption produces heat, and is soon an exothermic process. The positive value of ΔS found for SMT and for VGM showed that during the process of sorption, there is an increase in disorder of the system. The negative value for ΔS found for CSC indicates a decrease of randomness in solid–solution interface and no significant change occurs in the internal structure of biosorbent by adsorption of diuron.

The magnitude of the enthalpy change can be used to classify the type of interaction between the biosorbent and sorbate. According to the values of adsorption enthalpy obtained in this study, the biosorption of diuron by SMT, CSC and VGM biosorbents was due to physical adsorption, suggesting weak interactions between the biosorbents and diuron. Values of $\Delta H < 20$ kJ mol^{-1} indicates a physical adsorption [40]. For the kinetic study, the pseudo-second order model was the model that best represented the experimental data and this model is used to describe chemisorption. Thus, physical and chemical adsorption may be occurring.

4. Conclusions

The biosorption ability of diuron by *M. oleifera* seed, bark and pods was studied and the results indicated the potential application of biomaterials in water treatment. The SMT adsorbent removed 71% of diuron; CSC and VGM removed 74% and 73% of diuron from aqueous solution, respectively. The statistical analysis performed to verify which parameters were significant in the diuron biosorption by *M. oleifera* parts showed that the adsorption process with SMT was influenced by the amount of adsorbent mass, temperature and stirring speed; for the CSC, the adsorption process was influenced by the amount of adsorbent mass, pH and agitation speed and for VGM, by the amount of adsorbent mass and pH. For the three biosorbents, the highest removal efficiencies occurred in the solution with the lowest concentration of diuron, at the most basic pH, with the highest agitation

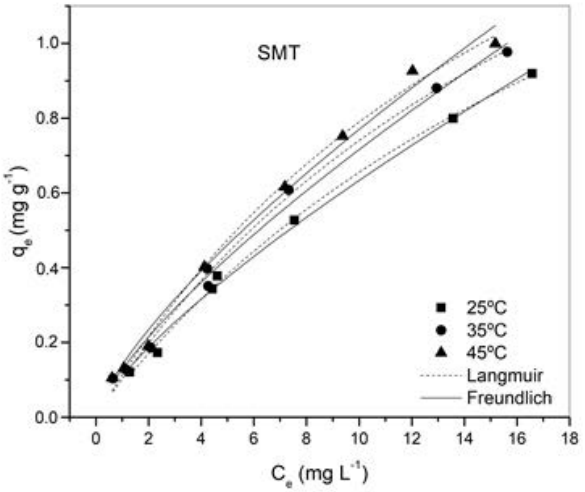

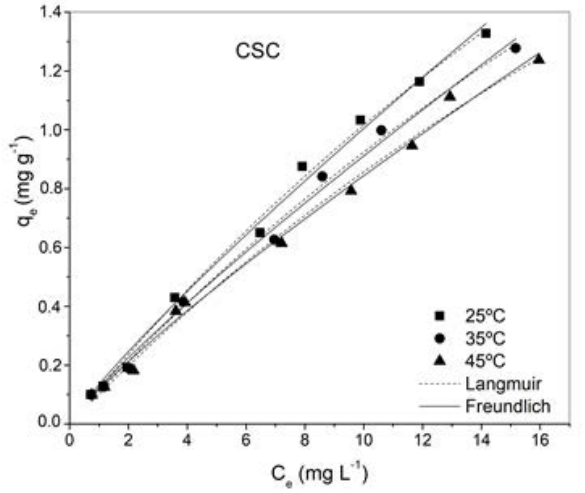

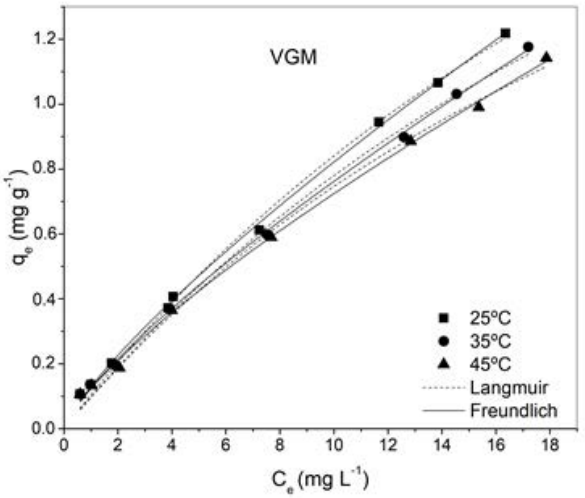

Fig. 6. Adsorption isotherms for SMT, CSC and VGM biosorbents by applying the Langmuir and Freundlich models at the temperatures of 25°C, 35°C and 45°C.

Table 6
Thermodynamic parameters of biosorption of diuron by SMT, CSC and VGM biosorbent

	SMT	CSC	VGM
ΔH (kJ mol^{-1})	11.93	–6.92	–0.92
ΔS (kJ mol^{-1} K^{-1})	0.056	–0.005	0.013
ΔG_{298K} (kJ mol^{-1})	–4.88	–5.43	–4.79
ΔG_{308K} (kJ mol^{-1})	–5.48	–5.38	–4.92
ΔG_{318K} (kJ mol^{-1})	–6.01	–5.33	–5.05
R^2	0.9976	0.9998	0.9996

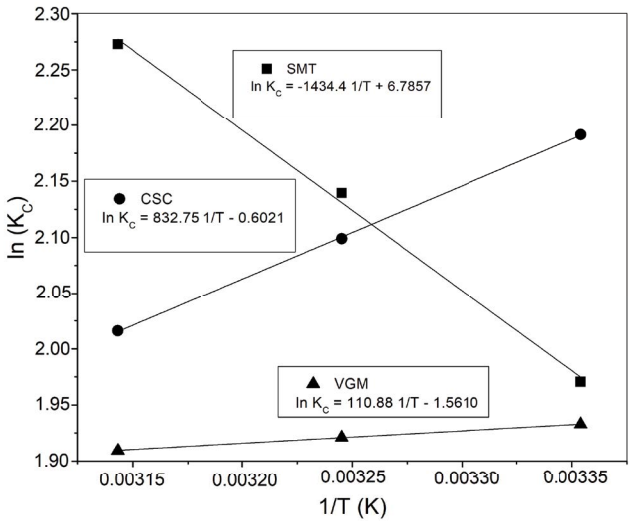

Fig. 7. Graph of ln K_c vs. 1/t for the estimation of thermodynamic parameters of biosorption of diuron by SMT, CSC and VGM biosorbent.

speed, the highest amount of biosorbent mass and biosorbent granulometry studied. In relation to temperature, for VGM and CSC the best biosorption occurred at 25°C, due to the process being spontaneous and exothermic; and for SMT at 45°C, because the process is spontaneous and endothermic. Based on the results, the SMT, CSC and VGM biosorbents are promising materials for the elimination of diuron from contaminated water.

Acknowledgements

To the Federal University of Sergipe for having granted *M. oleifera*. To National Council for Scientific and Technological Development (CNPq-Brazil) and Fundação Araucária (Brazil) for financial support.

References

[1] S. Giacomazzi, N. Cochet, Environmental impact of diuron transformation: a review, Chemosphere, 56 (2004) 1021–1032.
[2] G. Holmes, Australia's pesticide environmental risk assessment failure: the case of diuron and sugarcane, Mar. Pollut. Bull., 88 (2014) 7–13.

[3] W.A. Mitch, J.O. Sharp, R.R. Trussell, R.L. Valentine, L. Alvarez-Cohen, D.L. Sedlak, N-nitrosodimethylamine (NDMA) as a drinking water contaminant: a review. Environ. Eng. Sci., 20 (2003) 389–404.
[4] W.-H. Chen, T.M. Young, Influence of nitrogen source on NDMA formation during chlorination of diuron, Water Res., 43 (2009) 3047–3056.
[5] SINDIVEG, The sector of crop protection products in Brazil, 2016 [cited 2019 20/02]. Available from: http://sindiveg.org.br/importacoes-de-defensivos-agricolas-tem-aumento-no-primeiro-semestre-de-2016/.
[6] F.A. Petter, T.S. Ferreira, A.P. Sinhorin, F.A. Almeida, L.P. Pacheco, A.F. Silva, Biochar increases the sorption and reduces the potential contamination of subsurface water with diuron in sandy soil, Pedosphere, (2019), (In Press), https://doi.org/10.1016/S1002-0160(17)60434-X.
[7] R. Loos, G. Locoro, S. Comero, S. Contini, D. Schwesig, F. Werres, P. Balsaa, O. Gans, S. Weiss, L. Blaha, Pan-European survey on the occurrence of selected polar organic persistent pollutants in ground water, Water Res., 44 (2010) 4115–4126.
[8] C.C. Kaonga, K. Takeda, H. Sakugawa, Diuron, Irgarol 1051 and Fenitrothion contamination for a river passing through an agricultural and urban area in Higashi Hiroshima City, Japan. Sci. Total Environ., 518 (2015) 450–458.
[9] C. Directive, 98/83/EC on the quality of water intended for human consumption, Off. J. Eur. Communit, 330 (1998) 42.
[10] A. Di Bernardo Dantas, C. Paschoalato, M. Martinez, R. Ballejo, L. Di Bernardo, Removal of diuron and hexazinone from Guarany aquifer groundwater. Braz. J. Chem. Eng., 28 (2011) 415–424.
[11] C. Maqueda, M. Dos Santos Afonso, E. Morillo, R.T. Sánchez, M. Perez-Sayago, T. Undabeytia, Adsorption of diuron on mechanically and thermally treated montmorillonite and sepiolite. Appl. Clay Sci., 72 (2013) 175–183.
[12] S.R. Rissato, M. Libânio, G.P. Giafferis, M. Gerenutti, Determinação de pesticidas organoclorados em água de manancial, água potável e solo na região de Bauru (SP). Quim. Nova, 27 (2004) 739–743.
[13] I. Buchanan, H.C. Liang, Z.K. Liu, V. Razaviarani, M.Z. Rahman, Pesticides and herbicides, Water Environ. Res., 82 (2013) 1594–1693.
[14] S.-W. Nam, D.-J. Choi, S.-K. Kim, N. Her, K.-D. Zoh, Adsorption characteristics of selected hydrophilic and hydrophobic micropollutants in water using activated carbon, J. Hazard. Mater., 270 (2014) 144–152.
[15] V. Gupta, Application of low-cost adsorbents for dye removal–a review, J. Environ. Manage., 90 (2009) 2313–2342.
[16] A. Gebrekidan, M. Teferi, T. Asmelash, K. Gebrehiwet, A. Hadera, K. Amare, J. Deckers, B. Van Der Bruggen, *Acacia etbaica* as a potential low-cost adsorbent for removal of organochlorine pesticides from water, J. Water Resour. Prot., 7 (2015) 278.
[17] Z. Aksu, Application of biosorption for the removal of organic pollutants: a review, Process Biochem., 40 (2005) 997–1026.
[18] P. Kumari, P. Sharma, S. Srivastava, M. Srivastava, Biosorption studies on shelled *Moringa oleifera* Lamarck seed powder: removal and recovery of arsenic from aqueous system, Int. J. Miner. Process., 78 (2006) 131–139.
[19] M. Matouq, N. Jildeh, M. Qtaishat, M. Hindiyeh, M.Q. Al Syouf, The adsorption kinetics and modeling for heavy metals removal from wastewater by *Moringa* pods, J. Environ. Chem. Eng., 3 (2015) 775–784.
[20] S.N. do Carmo Ramos, A.L.P. Xavier, F.S. Teodoro, M.M.C. Elias, F.J. Goncalves, L.F. Gil, R.P. de Freitas, L.V.A. Gurgel, Modeling mono-and multi-component adsorption of cobalt (II), copper (II), and nickel (II) metal ions from aqueous solution onto a new carboxylated sugarcane bagasse. Part I: Batch adsorption study, Ind. Crops Prod., 74 (2015) 357–371.
[21] M. Akhtar, S.M. Hasany, M. Bhanger, S. Iqbal, Sorption potential of *Moringa oleifera* pods for the removal of organic pollutants from aqueous solutions, J. Hazard. Mater., 141 (2007) 546–556.
[22] A.T.A. Baptista, M.O. Silva, R.G. Gomes, R. Bergamasco, M.F. Vieira, A.M.S. Vieira, Protein fractionation of seeds of *Moringa oleifera* lam and its application in superficial water treatment, Sep. Purif. Technol., 180 (2017) 114–124.
[23] F.O. Tavares, L.A.d.M. Pinto, F.d.J. Bassetti, M.F. Vieira, R. Bergamasco, A.M.S. Vieira, Environmentally friendly biosorbents (husks, pods and seeds) from *Moringa oleifera* for Pb(II) removal from contaminated water, Environ. Technol., 38 (2017) 3145–3155.
[24] Z.F. Ma, J. Ahmad, H. Zhang, I. Khan, S. Muhammad, Evaluation of phytochemical and medicinal properties of Moringa (*Moringa oleifera*) as a potential functional food, S. Afr. J. Bot., (2019), (In Press), https://doi.org/10.1016/j.sajb.2018.12.002.
[25] C. Cui, S. Chen, X. Wang, G. Yuan, F. Jiang, X. Chen, L. Wang, Characterization of *Moringa oleifera* roots polysaccharide MRP-1 with anti-inflammatory effect, Int. J. Biol. Macromol., 132 (2019) 844–851.
[26] D. Rezende, L. Nishi, P.F. Coldebella, M.F. Silva, M.F. Vieira, A.M. Vieira, R. Bergamasco, M.R. Fagundes-Klen, Groundwater nitrate contamination: assessment and treatment using *Moringa oleifera* Lam. seed extract and activated carbon filtration, Can. J. Chem. Eng., 94 (2016) 725–732.
[27] D.H.K. Reddy, K. Seshaiah, A.V.R. Reddy, M.M. Rao, M.C. Wang, Biosorption of Pb^{2+} from aqueous solutions by *Moringa oleifera* bark: equilibrium and kinetic studies, J. Hazard. Mater., 174 (2010) 831–838.
[28] M.H. Kalavathy, L.R. Miranda, *Moringa oleifera*—A solid phase extractant for the removal of copper, nickel and zinc from aqueous solutions, Chem. Eng. J., 158 (2010) 188–199.
[29] J.J. Ojeda, M. Dittrich, Fourier transform infrared spectroscopy for molecular analysis of microbial cells, in Microbial Systems Biology 2012, Springer, pp. 187–211.
[30] A.M.S. Mimura, T.d.A. Vieira, P.B. Martelli, H.d.F. Gorgulho, Aplicação da casca de arroz na adsorção dos íons Cu^{2+}, Al^{3+}, Ni^{2+} e Zn^{2+}, Quim. Nova, 33 (2010) 1279–1284.
[31] V.K. Gupta, B. Gupta, A. Rastogi, S. Agarwal, A. Nayak, Pesticides removal from waste water by activated carbon prepared from waste rubber tire, Water Res., 45 (2011) 4047–4055.
[32] S.Y. Lagergren, Zur Theorie der sogenannten Adsorption gelöster Stoffe, 1898.
[33] Y. Ho, J. Ng, G. McKay, Kinetics of pollutant sorption by biosorbents: review, Sep. Purif. Rev., 29 (2000) 189–232.
[34] W. Weber, J. Morris, Kinetics of adsorption on carbon from solution, J. Sanit. Eng. Div. Am. Soc. Civ. Eng., 89 (1963) 31–60.
[35] G. Boyd, A. Adamson, L. Myers Jr, The exchange adsorption of ions from aqueous solutions by organic zeolites. II. Kinetics, J. Am. Chem. Soc., 69 (1947) 2836–2848.
[36] I. Langmuir, The constitution and fundamental properties of solids and liquids. Part I. Solids, J. Am. Chem. Soc., 38 (1916) 2221–2295.
[37] H. Freundlich, Over the adsorption in solution, J. Phys. Chem., 57 (1906) 1100–1107.
[38] M. Temkin, V. Pyzhev, Kinetics of ammonia synthesis on promoted iron catalyst, Acta Phys. Chim. USSR, 12 (1940) 327.
[39] M. Dubinin, The equation of the characteristic curve of activated charcoal, in Dokl. Akad. Nauk. SSSR. 55 (1947) 327–329.
[40] Y. Liu, Is the free energy change of adsorption correctly calculated?, J. Chem. Eng. Data, 54 (2009) 1981–1985.
[41] S. Salvestrini, V. Leone, P. Iovino, S. Canzano, S. Capasso, Considerations about the correct evaluation of sorption thermodynamic parameters from equilibrium isotherms, J. Chem. Thermodyn., 68 (2014) 310–316.
[42] C.S.T. Araújo, D.C. Carvalho, H.C. Rezende, I.L.S. Almeida, L.M. Coelho, N.M.M. Coelho, T.L. Marques, V.N. Alves, Bioremediation of Waters Contaminated with Heavy Metals Using *Moringa oleifera* Seeds as Biosorbent, in D.Y. Patil, Ed., Applied Bioremediation - Active and Passive Approaches, 2013.
[43] E. Ayranci, N. Hoda, E. Bayram, Adsorption of benzoic acid onto high specific area activated carbon cloth, J. Colloid Interface Sci., 284 (2005) 83–88.
[44] G. Sheng, Y. Yang, M. Huang, K. Yang, Influence of pH on pesticide sorption by soil containing wheat residue-derived char. Environ. Pollut., 134 (2005) 457–463.

[45] P. Rocha, A. Faria, L. Borges, L. Silva, A. Silva, E. Ferreira, Sorption and desorption of diuron in four brazilian latosols, Planta Daninha, 31 (2013) 231–238.
[46] M. Madhava Rao, A. Ramesh, G. Purna Chandra Rao, K. Seshaiah, Removal of copper and cadmium from the aqueous solutions by activated carbon derived from *Ceiba pentandra* hulls, J. Hazard. Mater., 129 (2006) 123–129.
[47] D.H.K. Reddy, D.K.V. Ramana, K. Seshaiah, A.V.R. Reddy, Biosorption of Ni(II) from aqueous phase by *Moringa oleifera* bark, a low cost biosorbent, Desalination, 268 (2011) 150–157.
[48] J. Pan, B. Guan, Adsorption of nitrobenzene from aqueous solution on activated sludge modified by cetyltrimethylammonium bromide, J. Hazard. Mater., 183 (2010) 341–346.
[49] L. Mataka, S. Sajidu, W. Masamba, J. Mwatseteza, Cadmium Sorption by *Moringa stemopetala* and *Moringa oleifera* Seed Powders: Batch, Time, Temperature, pH and Adsorption Isotherm Studies, Acad. J., 2010.
[50] G. McKay, M.S. Otterburn, A.G. Sweeney, The removal of colour from effluent using various adsorbents—III. Silica: Rate processes. Water Res., 14 (1980) 15–20.
[51] J. Febrianto, A.N. Kosasih, J. Sunarso, Y.-H. Ju, N. Indraswati, S. Ismadji, Equilibrium and kinetic studies in adsorption of heavy metals using biosorbent: a summary of recent studies, J. Hazard. Mater., 162 (2009) 616–645.
[52] D.D. Maksin, S.O. Kljajević, M.B. Đolić, J.P. Marković, B.M. Ekmeščić, A.E. Onjia, A.B. Nastasović, Kinetic modeling of heavy metal sorption by vinyl pyridine based copolymer, Hem. Ind., 66 (2012) 795–804.
[53] A. Ebrahimi, M. Ehteshami, B. Dahrazma, Isotherm and kinetic studies for the biosorption of cadmium from aqueous solution by *Alhaji maurorum* seed, Process Saf. Environ. Prot., 98 (2015) 374–382.
[54] S. Srivastava, S.B. Agrawal, M.K. Mondal, Biosorption isotherms and kinetics on removal of Cr(VI) using native and chemically modified *Lagerstroemia speciosa* bark, Ecol. Eng., 85 (2015) 56–66.
[55] F. Wang, L. Tan, Q. Liu, R. Li, Z. Li, H. Zhang, S. Hu, L. Liu, J. Wang, Biosorption characteristics of Uranium (VI) from aqueous solution by pollen pini, J. Environ. Radioact., 150 (2015) 93–98.
[56] D.O. Cooney, Adsorption Design for Wastewater Treatment, CRC Press, 1998.